Performance Analysis of Cell-Free Massive MIMO Over Spatially Correlated Fading Channels

Wen Fan*, Jiayi Zhang*, Emil Björnson†, Shuaifei Chen*, and Zhangdui Zhong‡
*School of Electronic and Information Engineering, Beijing Jiaotong University, Beijing 100044, China
†Department of Electrical Engineering (ISY), Linköping University, Linköping, Sweden
‡State Key Laboratory of Rail Traffic Control and Safety, Beijing Jiaotong University, Beijing 100044, China

***Abstract*—Cell-free massive multiple-input multiple-output (MIMO) is a promising network architecture for future wireless systems. This paper investigates the uplink performance of cell-free massive MIMO systems employing the least-square (LS) estimator over spatially correlated fading channels. We first derive a generalized closed-form expression of the spectral efficiency as a function of the number of access point (AP) antennas and the spatial correlation matrices. We use this result to analyze the impact that the fronthaul, number of users and number of APs have on the energy efficiency. Compared to traditional co-located massive MIMO using maximum ratio combining (MRC), our analysis shows that the large performance gain of cell-free massive MIMO with low-complexity linear LS estimators.**

I. Introduction

The demand for data throughput has been exponentially increasing for decades due to a large number of users and many kinds of wireless applications [1]. To meet this demand, cell-free massive MIMO has been proposed in [2]. As a practical embodiment of network MIMO, cell-free massive MIMO employs hundreds or even thousands of geographically distributed APs over a wide area to jointly provide access to data transmission to several users based only on local channel state information (CSI). Similar to co-located massive MIMO [3], the channel hardening and favorable propagation properties can be utilized in cell-free massive MIMO using many antennas per AP and spatially well separated users [4].

Recently, a plethora of papers in the field of cell-free massive MIMO has been published. In [2], [5], the uplink and downlink spectral efficiency (SE) of cell-free massive MIMO with conjugate beamforming or zero forcing was derived, respectively. These papers quantitatively show the significant performance improvement over small-cell systems. In [6], [7], the spectral and energy efficiency expressions of cell-free massive MIMO with hardware impairments was derived. The SE of cell-free massive MIMO improves significantly with the receiver filter coefficient design and power allocation [8], [9]. The SE can be further improved by employing the non-orthogonal multiple-access technique in the regime of large number of users [10]. Taking into account the fronthaul energy consumption, the energy efficiency (EE) has been investigated with conjugate beamforming and zero-forcing precoder [11], [12]. Compared to co-located massive MIMO, an order of magnitude higher EE can be achieved in cell-free massive MIMO, while ensuring uniformly good service for all users in an urban deployment of 64 service antennas and 18 users randomly distributed inside a circle with 0.5 km radius [13]. Furthermore, the authors in [14] investigated the transmission of system information in a cell-free massive MIMO system.

All the above-cited papers assumed that the APs have only one antenna or the channels to the multiple antennas at the APs are mutually independent. However, due to the limited physical space and the finite number of scattering clusters, the practical channels are spatially correlated [15]. Moreover, many previous papers assume that the minimum mean-square error (MMSE) channel estimation is utilized at the APs. In practical, it is difficult to obtain prior statistical information owing to rapid channel variations. To address this shortcoming, the LS estimator can be utilized which does not require any statistical information [16].

Motivated by the aforementioned discussion, we consider cell-free massive MIMO with LS estimators over spatially correlated fading channels. Rigorous closed-form SE and EE expressions are derived by using the use-and-then-forget (UatF) methodology. For a large number of APs, we show that the effects of spatial correlation, inter-user interference, and noise disappear. Our results reveal that one can achieve both large SE and EE by setting appropriate system parameters, e.g., the number of antennas at each AP and the number of served APs. In a propagation environment with spatially correlation, it is interesting to reveal that a large performance gain is offered by cell-free massive MIMO than the one of co-located massive MIMO using MRC.

II. System Model

Let us consider a cell-free massive MIMO system in which M APs serve K users in the same wireless resource. There are N antennas in each AP and a single antenna in each user. It is assumed that APs and users are arbitrarily distributed over a large area. In addition, all APs are connected to a central processing unit (CPU) via a fronthaul link. The channels remain constant in a coherence time-frequency block of τ_c samples, and take independent random realizations in each

This work was supported in part by National Key Research and Development Program (Nos. 2016YFE0200900 and 2016YFB1200102-04), National Natural Science Foundation of China (Nos. 61601020, 61725101 and U1834210), the Beijing Natural Science Foundation (Nos. 4182049, L171005 and L172020), the open research fund of National Mobile Communications Research Laboratory, Southeast University (No. 2018D04), Key Laboratory of Optical Communication and Networks (No. KLOCN2018002), and Major projects of Beijing Municipal Science and Technology Commission (No. Z181100003218010).

978-1-5386-8088-9/19/$31.00 ©2019 IEEE

block. We consider the uplink, using the duration of τ_{p} samples for uplink training and the remaining $\tau_{\mathrm{u}} = \tau_{\mathrm{c}} - \tau_{\mathrm{p}}$ samples for the uplink data transmission.

In this paper, we consider spatially correlated Rayleigh fading channels, since practical channels are always correlated [16]. The spatially correlated channel vector between the mth AP and the kth user $\mathbf{g}_{mk} \in \mathbb{C}^{N\times 1}$, $m = 1,\ldots,M, k = 1,\ldots,K$, is given by

$$\mathbf{g}_{mk} = \beta_{mk}^{1/2}\mathbf{h}_{mk}, \tag{1}$$

where β_{mk} denotes the large-scale fading that is independent of the AP's antenna index and $\mathbf{h}_{mk} \in \mathbb{C}^{N\times 1}$ denotes the vector of small-scale fading coefficients between the mth AP and the kth user. We concentrate on correlated small-scale fading vector such that $\mathbf{h}_{mk} \sim \mathcal{CN}(\mathbf{0}_N, \mathbf{R}_{mk})$, where $\mathbf{R}_{mk} \in \mathbb{C}^{N\times N}$ is the positive semi-definite spatial correlation matrix describing the channel correlation, including the antenna gains and radiation patterns at the transmitter and receiver. Moreover, we normalize $\mathbf{R}_{mk}$ as $\mathrm{tr}(\mathbf{R}_{mk})/N = 1$.

A. Uplink Training

During the uplink training phase, all users send their pilot sequences to all APs at the same time. The AP utilizes the received pilot sequence signals to estimate the channels. We denote by $\sqrt{\tau_{\mathrm{p}}}\boldsymbol{\varphi}_k \in \mathbb{C}^{\tau_{\mathrm{p}}\times 1}$, where $\|\boldsymbol{\varphi}_k\|^2 = 1$, $k = 1,...,K$ the pilot sequence of the kth user. Then, the received pilot matrix $\mathbf{Y}_{\mathrm{p},m} \in \mathbb{C}^{N\times\tau_p}$ at the mth AP is expressed as

$$\mathbf{Y}_{\mathrm{p},m} = \sqrt{\rho\tau_{\mathrm{p}}}\sum_{k=1}^{K}\mathbf{g}_{mk}\boldsymbol{\varphi}_k^H + \mathbf{W}_{\mathrm{p},m}, \tag{2}$$

where ρ is the normalized transmission signal to noise ratio (SNR) of each pilot sequence, $\mathbf{W}_{\mathrm{p},m} \in \mathbb{C}^{N\times\tau_{\mathrm{p}}}$ is the additive noise matrix which has independent and identically distributed (i.i.d.) $\mathcal{CN}(0,1)$ components. We assume $\tau_{\mathrm{p}} = K$ and choose $\boldsymbol{\varphi}_1, \boldsymbol{\varphi}_2, ..., \boldsymbol{\varphi}_k$ as pairwisely orthogonal [17]. The pilot contamination induced by $\tau_{\mathrm{p}} < K$ can be handled by the same techniques as described in this paper, but the analysis is more lengthy and therefore omitted due to space limitations.

In order to estimate the channel vector $\mathbf{g}_{mk}$, the AP first conducts a de-spreading operation through the inner product between $\mathbf{Y}_{\mathrm{p},m}$ and $\boldsymbol{\varphi}_k$ as

$$\breve{\mathbf{y}}_{\mathrm{p},mk} \triangleq \mathbf{Y}_{\mathrm{p},m}\boldsymbol{\varphi}_k = \sqrt{\rho\tau_{\mathrm{p}}}\mathbf{g}_{mk} + \tilde{\mathbf{w}}_{\mathrm{p},mk}, \tag{3}$$

where $\tilde{\mathbf{w}}_{\mathrm{p},mk} = \mathbf{W}_{\mathrm{p},m}\boldsymbol{\varphi}_k$. due to $\|\boldsymbol{\varphi}_k\|^2 = 1$, then $\tilde{\mathbf{w}}_{\mathrm{p},mk} \sim \mathcal{CN}(\mathbf{0}_N, \mathbf{I}_N)$. In practice, it can be hard to estimate the spatial correlation matrices. So we choose the LS estimator in the performance analysis of the cell-free massive MIMO since it requires no prior statistical information and has low computational complexity. The LS estimation is defined as the value of $\hat{\mathbf{g}}_{mk}$ that minimizes $\|\breve{\mathbf{y}}_{\mathrm{p},mk} - \sqrt{\rho\tau_{\mathrm{p}}}\hat{\mathbf{g}}_{mk}\|^2$, that is

$$\hat{\mathbf{g}}_{mk} = \frac{1}{\sqrt{\rho\tau_{\mathrm{p}}}}\breve{\mathbf{y}}_{\mathrm{p},mk} = \mathbf{g}_{mk} + \frac{1}{\sqrt{\rho\tau_{\mathrm{p}}}}\tilde{\mathbf{w}}_{\mathrm{p},mk}. \tag{4}$$

B. Uplink Data Transmission

During the uplink, all K users transmit their data to the APs at the same time and frequency. Before transmitting the data, the kth user weighs its symbol q_k, $\mathbb{E}\left\{|q_k|^2\right\} = 1$, by a power control coefficient $\sqrt{\eta_k}$, $0 \leqslant \eta_k \leqslant 1$. The signal received at the mth AP is

$$\mathbf{y}_{\mathrm{u},m} = \sqrt{\rho}\sum_{k=1}^{K}\sqrt{\eta_k}\mathbf{g}_{mk}q_k + \mathbf{w}_{\mathrm{u},m}, \tag{5}$$

where $\rho\eta_k$ the normalized uplink SNR of the kth user and $\mathbf{w}_{\mathrm{u},m}$ is additive noise at the mth AP, as $\mathbf{w}_{\mathrm{u},m} \sim \mathcal{CN}(\mathbf{0}_N, \mathbf{I}_N)$.

To detect the symbol transmitted from the kth user, q_k, we use MRC, i.e., the inner product between received signal $\mathbf{y}_{\mathrm{u},m}$ and channel estimate $\hat{\mathbf{g}}_{mk}$, and send the so-obtained quantity $\hat{\mathbf{g}}_{mk}^H\mathbf{y}_{\mathrm{u},m}$ to the CPU via an infinite-precision fronthaul link. Then, the CPU is putting these signals together to form

$$\begin{aligned} r_{\mathrm{u},k} &= \sum_{m=1}^{M}\hat{\mathbf{g}}_{mk}^H\mathbf{y}_{\mathrm{u},m} \\ &= \sqrt{\rho}\sum_{k'=1}^{K}\sum_{m=1}^{M}\sqrt{\eta_{k'}}\hat{\mathbf{g}}_{mk}^H\mathbf{g}_{mk'}q_{k'} + \sum_{m=1}^{M}\hat{\mathbf{g}}_{mk}^H\mathbf{w}_{\mathrm{u},m}. \end{aligned} \tag{6}$$

Finally, q_k is detected by $r_{\mathrm{u},k}$.

III. Performance Analysis

A. SE Analysis

In this section, we first derive a closed-form expression of the uplink SE of cell-free massive MIMO systems over spatially correlated Rayleigh fading channels for finite M. The CPU detects the desired signal q_k from $r_{\mathrm{u},k}$ in (6). Using the analysis method in [18], we rewrite the received signal $r_{\mathrm{u},k}$ as

$$r_{\mathrm{u},k} = \mathrm{DS}_k \cdot q_k + \mathrm{BU}_k \cdot q_k + \sum_{k'\neq k}^{K}\mathrm{UI}_{kk'} \cdot q_{k'} + \mathrm{NI}_k, \tag{7}$$

where

$$\mathrm{DS}_k \triangleq \sqrt{\rho\eta_k}\mathbb{E}\left\{\sum_{m=1}^{M}\hat{\mathbf{g}}_{mk}^H\mathbf{g}_{mk}\right\}, \tag{8}$$

$$\mathrm{BU}_k \triangleq \sqrt{\rho\eta_k}\left(\sum_{m=1}^{M}\hat{\mathbf{g}}_{mk}^H\mathbf{g}_{mk} - \mathbb{E}\left\{\sum_{m=1}^{M}\hat{\mathbf{g}}_{mk}^H\mathbf{g}_{mk}\right\}\right), \tag{9}$$

$$\mathrm{UI}_{kk'} \triangleq \sqrt{\rho}\sum_{m=1}^{M}\sqrt{\eta_{k'}}\hat{\mathbf{g}}_{mk}^H\mathbf{g}_{mk'}, \tag{10}$$

$$\mathrm{NI}_k \triangleq \sum_{m=1}^{M}\hat{\mathbf{g}}_{mk}^H\mathbf{w}_{\mathrm{u},m}, \tag{11}$$

denote the desired signal (DS), the beamforming uncertainty gain (BU), multiuser interference (UI), and the noise interference (NI), respectively. Then, the corresponding uplink SINR

of the kth user is expressed as

$$\mathrm{SINR}_k=\frac{|\mathrm{DS}_k|^2}{\mathbb{E}\left\{|\mathrm{BU}_k|^2\right\}+\sum\limits_{k'\neq k}^{K}\mathbb{E}\left\{|\mathrm{UI}_{kk'}|^2\right\}+\mathbb{E}\left\{|\mathrm{NI}_k|^2\right\}}. \quad (12)$$

Theorem 1. *The SE of the cell-free massive MIMO with the LS estimator over spatially correlated Rayleigh channels is given by* (13) *at the bottom of the next page.*

Proof: Please refer to Appendix. ■

Remark: Following the similar method in Lemma 1, we can derive the SE of the co-located massive MIMO with the LS estimator over spatially correlated Rayleigh channels as (14) at the bottom of the next page, which is precisely the uplink SE lower bound of a co-located massive MIMO system obtained in [19]. For this purpose, we assume the base station with co-located MN service antennas is located at the center of the region, where K UEs are randomly distributed inside the region. We use β_k to denote the large-scale fading coefficient and $\mathbf{R}_k$ to represent the spatial correlation vector in co-located systems, respectively. Note that the size of $\mathbf{R}_k$ is $MN\times MN$, while $\mathbf{R}_{mk}$ is $N\times N$ for cell-free massive MIMO.

B. EE Analysis

The EE is defined as the sum throughput divided by the total energy consumption in the network. We consider a widely used model of energy consumption [11], which includes contributions from transceivers and fronthaul. More precisely, the total energy consumption model is given by

$$P_{\text{total}}=\sum_{k=1}^{K}P_k+\sum_{m=1}^{M}NP_{\text{tc},m}+\sum_{m=1}^{M}P_{\text{fh},m}\,, \quad (15)$$

where P_m represents the circuit power consumption that includes analog transceiver components and digital signal processing at the mth AP, $P_{\text{fh},m}$ denotes the power consumption of the fronthaul link between the CPU and the mth AP, and P_k is the transmitted power consumed by the kth UE. The circuit power consumption is given by $NP_{\text{tc},m}$, where $P_{\text{tc},m}$ is the internal power of running the circuit components associated with each antenna of the mth AP. Then, the fronthaul power consumption $P_{\text{fh},m}$ can be modeled as

$$P_{\text{fh},m}=P_{0,m}+B\cdot\sum_{k=1}^{K}\mathrm{SE}_k\cdot P_{\text{bt},m}, \quad (16)$$

where $P_{0,m}$ represents a fixed power consumption of each fronthaul depending on the distances between the APs and the CPU and the topology of the system, $P_{\text{bt},m}$ is the power consumption related to traffic, and B denotes the system bandwidth. Finally, we assume the power consumption P_k is constant for all K users. Therefore, we can derive the expression of EE as

$$\mathrm{EE}\ =B\cdot\sum_{k=1}^{K}\mathrm{SE}_k/P_{\text{total}}. \quad (17)$$

TABLE I
KEY SIMULATION PARAMETERS

Parameters	Value
Transmit powers: $\bar{\rho}$	0.1 W
Noise figure: n_f	9 dB
System bandwidth: B	20 MHz
Power control coefficient: η_k	1
$P_{\text{tc},m}$	0.2 W
$P_{0,m}$	0.825 W
$P_{\text{bt},m}$	0.25 W/Gbits/s
k_B	1.381×10^{-23} J per K
T_0	290 K

IV. NUMERICAL RESULTS AND DISCUSSIONS

In this section, numerical results are provided to quantitatively analyze the system performance in terms of uplink spectral and EE. We assume that the M APs and K users are independently and uniformly distributed within a square of size 1×1 km^2. The large-scale fading coefficient β_{mk} is modeled (in dB) in [15] as

$$\beta_{mk}=-34.53-38\log_{10}\left(d_{mk}/1\,\mathrm{m}\right)+F_{mk}, \quad (18)$$

where d_{mk} is the distance between the mth AP and the kth user, and $F_{mk}\sim\mathcal{N}\left(0,100\right)$ is shadow fading. As for the correlation matrix $\mathbf{R}_{mk}$, we consider the widely used local scattering model with Gaussian angular distribution [16]. $\mathbf{R}_{mk}$ is Toeplitz matrix, and the $(l,\ n)$th element of $\mathbf{R}_{mk}$ can be computed by [16, Eq.(2.23)]

$$[\mathbf{R}_{mk}]_{l,n}=\int_{20\sigma_\varphi}^{20\sigma_\varphi}e^{2\pi jd_H(l-n)\sin(\varphi+\delta)}\frac{1}{\sqrt{2\pi}\sigma_\varphi}e^{-\frac{\delta^2}{2\sigma_\varphi^2}}d\delta, \quad (19)$$

where the nominal angle φ is randomly chosen between $-\pi$ to π, and σ_φ is called the angular standard deviation (ASD) determining how large the deviations from the nominal angle are. In this paper, we use $\sigma_\varphi=10^\circ$ to represent strong spatial correlation and $\sigma_\varphi=30^\circ$ to represent moderate spatial correlation. $\mathbf{R}_{mk}$ is expressed as $\mathbf{R}_{mk}=\mathbf{I}_N$ in the special uncorrelated Rayleigh fading case, and this case is considered for comparison in the following. Other simulation parameters are summarized in Table I, which are provided in [2], [11].

First, we analyze the effect of spatial correlation on the SE. The numerical and analytical average SE are compared in Fig. 1, as a function of the number of APs (M) and antennas per AP (N). Here we choose $K=10$. It is clear that the analytical and simulated curves overlap for all considered cases. The average SE is an increasing function of M. The SE increases when the numbers of N increases for the case of the same number of M. In addition, it can be seen from Fig. 2 that the SE over the uncorrelated Rayleigh fading channels is better than with correlated Rayleigh fading channels. Furthermore, we observe that the performance gap between uncorrelated Rayleigh fading channels and correlated Rayleigh fading channels increases as the number of M and

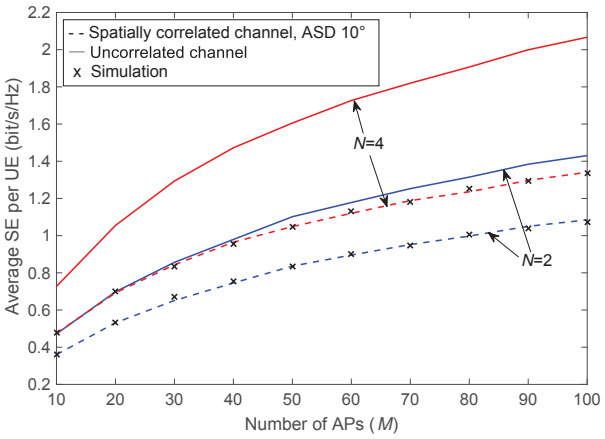

Fig. 1. Average SE of cell-free massive MIMO systems over spatially correlated and uncorrelated Rayleigh fading channels against the number of APs M for $K = 10$.

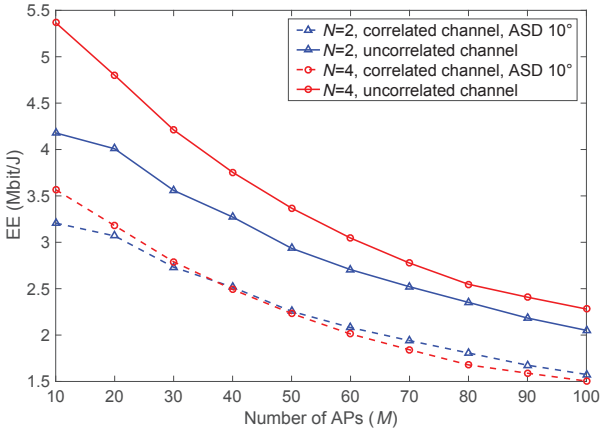

Fig. 3. EE of cell-free massive MIMO systems over spatially correlated and uncorrelated Rayleigh fading channels against the number of APs M for $K = 10$.

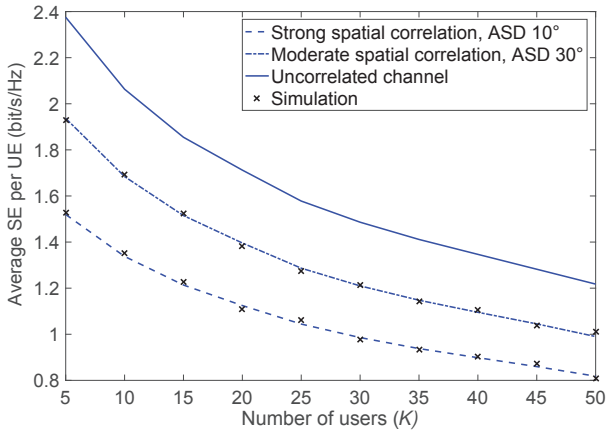

Fig. 2. Average SE of cell-free massive MIMO systems over spatially correlated and uncorrelated Rayleigh fading channels against the number of users K for $M = 100$ and $N = 4$.

N increases. Therefore, for a large number of APs in a cell-free massive MIMO system, the spatial correlation will be an important factor affecting the SE in practice.

Fig. 2 shows the average SE as a function of the number of users K with $M = 100$. The average SE is a decreasing function of K regardless of the strength of the spatial correlation. As can be obtained from (13), the larger number of users induces stronger inter-user interference, thus the SE declines but the sum SE may increase. As anticipated, the performance of the system with uncorrelated Rayleigh fading channels is better than the one of the channels with moderate or strong spatial correlation, and the performance of system over the channels with strong spatial correlation is worst for the considered case. This verifies that the system performance degradation is more serious when the spatial correlation is stronger.

Next, we analyze the effect of spatial correlation on EE. Fig. 3 investigates the EE as a function of the number of APs M. We choose $K = 10$ and $P_k = 1$ W. The first observation is that the EE is decreasing as the number of

$$\mathrm{SE}_k^{\mathrm{cf}} = \left(1-\frac{\tau_{\mathrm{p}}}{\tau_{\mathrm{c}}}\right)\log_2\left(1+\frac{\rho\eta_k\left|\sum\limits_{m=1}^{M}\beta_{mk}\mathrm{tr}\left(\mathbf{R}_{mk}\right)\right|^2}{\rho\sum\limits_{k'=1}^{K}\eta_{k'}\sum\limits_{m=1}^{M}\beta_{mk}\beta_{mk'}\mathrm{tr}\left(\mathbf{R}_{mk}\mathbf{R}_{mk'}\right)+\frac{1}{\tau_{\mathrm{p}}}\sum\limits_{k'=1}^{K}\eta_{k'}\sum\limits_{m=1}^{M}\beta_{mk'}\mathrm{tr}\left(\mathbf{R}_{mk'}\right)+\sum\limits_{m=1}^{M}\beta_{mk}\mathrm{tr}\left(\mathbf{R}_{mk}\right)+\frac{MN}{\rho\tau_{\mathrm{p}}}}\right). \tag{13}$$

$$\mathrm{SE}_k^{\mathrm{co}} = \left(1-\frac{\tau_{\mathrm{p}}}{\tau_{\mathrm{c}}}\right)\log_2\left(1+\frac{\rho\eta_k\left|\beta_k\mathrm{tr}\left(\mathbf{R}_k\right)\right|^2}{\rho\beta_k\sum\limits_{k'=1}^{K}\eta_{k'}\beta_{k'}\mathrm{tr}\left(\mathbf{R}_k\mathbf{R}_{k'}\right)+\frac{1}{\tau_{\mathrm{p}}}\sum\limits_{k'=1}^{K}\eta_{k'}\beta_{k'}\mathrm{tr}\left(\mathbf{R}_{k'}\right)+\beta_k\mathrm{tr}\left(\mathbf{R}_k\right)+\frac{MN}{\rho\tau_{\mathrm{p}}}}\right). \tag{14}$$

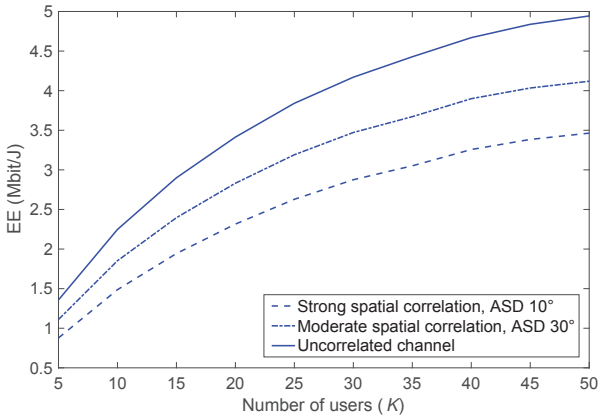

Fig. 4. EE of cell-free massive MIMO systems over spatially correlated and uncorrelated Rayleigh fading channels against the number of users K for $M = 100$ and $N = 4$.

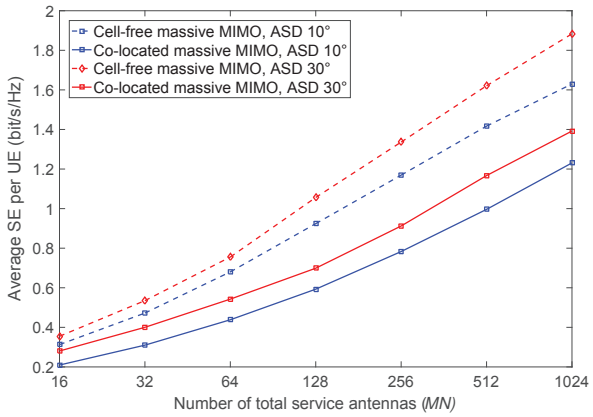

Fig. 5. Average SE of cell-free and co-located massive MIMO systems over spatially correlated Rayleigh fading channels against the number of total antennas MN for $K = 10$ and $N = 2$.

M increases under both fading channels. This results from the fact that the SE of one user is only related to a few APs, so increasing the number of APs results in more power consumption than the increase in SE. Similarly, the system performance over the uncorrelated Rayleigh fading channel is better than the one over the correlated Rayleigh fading channel. And the performance gap between uncorrelated and correlated Rayleigh channels decreases as the number of M increases. Furthermore, compared with Fig. 1, the trend of SE and EE is opposite with the increase of M. This indicates that the performance of SE and EE are mutually restricted. It can be concluded that in order to achieve larger EE and SE at the same time, the number of the APs need to be selected carefully. Fig. 3 also shows that one should increase M and K jointly to keep or increase the EE.

Fig. 4 shows the EE as a function of the number of users K with $M = 100$ and $N = 4$. The EE increases as K increases despite the strength of spatial correlation. The reason is that when M is much larger than K in cell-free massive MIMO, the power consumption of APs and users is almost the same. The traffic-dependent fronthaul power consumption decreases rapidly, while the sum SE might decreases more slowly. Therefore, serving more users at the same time improves the performance of EE. Likewise, the performance of the system over uncorrelated Rayleigh fading channels is better than the one of the channels with moderate or strong spatial correlation, and the performance of system over the channels with strong spatial correlation is worst for the considered case. To sum up, spatial correlation seriously affects the system performance and there is a trade-off between SE and EE.

Finally, we compared the SE of cell-free and co-located massive MIMO systems over spatially correlated Rayleigh fading channels in Fig. 5. The total number of service antennas is MN for both systems. We note that there is a large SE performance gap between the cell-free and co-located massive MIMO system in a spatially correlated scenario by using MRC. Compared to cellular massive MIMO, the spatial channel correlation at APs further reduces the level of channel hardening for cell-free massive MIMO. This is due to the fact that distributed APs can increase the condition number of the correlation matrices in the scenario with finite number of scattering clusters. With MRC, the co-located case is subject to massive interference from all antennas, while the cell-free case only leads to strong interference from a subset of the antennas. Therefore, we can conclude that the cell-free architecture can greatly improve the SE of the massive MIMO system over the correlated channels compared with the co-located architecture.

V. Conclusion

In this paper, we analyzed the uplink performance of cell-free massive MIMO, taking into account the effects of the spatial channel correlation when each AP is equipped with multiple antennas. Using the simple LS estimator, we derived rigorous closed-form expressions for the SE and analyzed the trend of EE under certain simulated values. The results show that the performance of the considered system decreases in the correlated Rayleigh fading channel in terms of SE and EE. In addition, we have to adjust the number of APs to balance the performance of SE and EE for different numbers of users on the condition that the number of APs is much larger than the number of users. In the future, we will consider the pilot contamination and other signal combining methods at the APs.

Appendix A

With the help of $\hat{\mathbf{g}}_{mk} = \mathbf{g}_{mk} + \frac{1}{\sqrt{\rho\tau_{\mathrm{p}}}}\tilde{\mathbf{w}}_{\mathrm{p},mk}$, we have

$$\mathrm{DS}_k = \sqrt{\rho\eta_k}\sum_{m=1}^{M}\mathbb{E}\left\{\left(\mathbf{g}_{mk} + \frac{1}{\sqrt{\rho\tau_{\mathrm{p}}}}\tilde{\mathbf{w}}_{\mathrm{p},mk}\right)^H\mathbf{g}_{mk}\right\}$$
$$\underline{\underline{(a)}}\ \sqrt{\rho\eta_k}\sum_{m=1}^{M}\mathbb{E}\left\{\mathbf{g}_{mk}^H\mathbf{g}_{mk}\right\}\underline{\underline{(b)}}\ \sqrt{\rho\eta_k}\sum_{m=1}^{M}\beta_{mk}\mathrm{tr}\left(\mathbf{R}_{mk}\right), \tag{20}$$

where (a) follows from the fact that $\mathbf{g}_{mk}$ and $\tilde{\mathbf{w}}_{\mathrm{p},mk}$ are independent, while (b) utilizes $\mathbf{h}_{mk} \sim \mathcal{CN}(\mathbf{0}_N, \mathbf{R}_{mk})$ and the following rules: $\mathbf{x}^H\mathbf{y} = \mathrm{tr}(\mathbf{y}^H\mathbf{x})$ for any vectors $\mathbf{x}$, $\mathbf{y}$.

Next, we compute $\mathbb{E}\left\{|\mathrm{BU}_k|^2\right\}$. From (9), we have

$$\begin{aligned}
&\mathbb{E}\left\{|\mathrm{BU}_k|^2\right\} \\
&\underline{\underline{(c)}}\ \rho\eta_k \sum_{m=1}^{M}\left(\mathbb{E}\left\{\left|\hat{\mathbf{g}}_{mk}^H\mathbf{g}_{mk}\right|^2\right\} - \left|\mathbb{E}\left\{\hat{\mathbf{g}}_{mk}^H\mathbf{g}_{mk}\right\}\right|^2\right) \\
&\underline{\underline{(d)}}\ \rho\eta_k \sum_{m=1}^{M}\left(\mathbb{E}\left\{\left|\hat{\mathbf{g}}_{mk}^H\mathbf{g}_{mk}\right|^2\right\} - \left|\beta_{mk}\mathrm{tr}\left(\mathbf{R}_{mk}\right)\right|^2\right), \quad (21)
\end{aligned}$$

where in (c) we have used

$$\mathbb{E}\left\{\left(\hat{\mathbf{g}}_{mk}^H\mathbf{g}_{mk} - \mathbb{E}\left\{\hat{\mathbf{g}}_{mk}^H\mathbf{g}_{mk}\right\}\right)\left(\hat{\mathbf{g}}_{m'k}^H\mathbf{g}_{m'k} - \mathbb{E}\left\{\hat{\mathbf{g}}_{mk}^H\mathbf{g}_{m'k}\right\}\right)^H\right\} = 0,$$

for $m \neq m'$, and in (d) we utilize the result of (20). Then

$$\begin{aligned}
&\mathbb{E}\left\{\left|\hat{\mathbf{g}}_{mk}^H\mathbf{g}_{mk}\right|^2\right\} = \mathbb{E}\left\{\left|\left(\mathbf{g}_{mk} + \frac{1}{\sqrt{\rho\tau_\mathrm{p}}}\tilde{\mathbf{w}}_{\mathrm{p},mk}\right)^H\mathbf{g}_{mk}\right|^2\right\} \\
&\underline{\underline{(e)}}\ \mathbb{E}\left\{\left|\mathbf{g}_{mk}^H\mathbf{g}_{mk}\right|^2\right\} + \frac{1}{\rho\tau_\mathrm{p}}\mathbb{E}\left\{\left|\tilde{\mathbf{w}}_{\mathrm{p},mk}^H\mathbf{g}_{mk}\right|^2\right\} \\
&\underline{\underline{(f)}}\ \left|\beta_{mk}\mathrm{tr}\left(\mathbf{R}_{mk}\right)\right|^2 + \beta_{mk}^2\mathrm{tr}\left(\mathbf{R}_{mk}^2\right) + \frac{\beta_{mk}}{\rho\tau_\mathrm{p}}\mathrm{tr}\left(\mathbf{R}_{mk}\right), \quad (22)
\end{aligned}$$

where in (e) we have used the fact in (a), while (f) can be obtained with the aid of Lemma 2 in [20] owing to $\mathbf{h}_{mk} \sim \mathcal{CN}(\mathbf{0}_N, \mathbf{R}_{mk})$ and $\tilde{\mathbf{w}}_{\mathrm{p},mk} \sim \mathcal{CN}(\mathbf{0}_N, \mathbf{I}_N)$.

Substitution of (22) into (21) yields

$$\mathbb{E}\left\{|\mathrm{BU}_k|^2\right\} = \rho\eta_k\sum_{m=1}^{M}\beta_{mk}^2\mathrm{tr}\left(\mathbf{R}_{mk}^2\right) + \frac{\eta_k}{\tau_\mathrm{p}}\sum_{m=1}^{M}\beta_{mk}\mathrm{tr}\left(\mathbf{R}_{mk}\right).$$

Then, we compute $\mathbb{E}\left\{|\mathrm{UI}_{kk'}|^2\right\}$. From (10), we have

$$\begin{aligned}
&\mathbb{E}\left\{|\mathrm{UI}_{kk'}|^2\right\} \\
&\underline{\underline{(g)}}\ \rho\eta_{k'}\mathbb{E}\left\{\left|\sum_{m=1}^{M}\mathbf{g}_{mk}^H\mathbf{g}_{mk'}\right|^2 + \left|\frac{1}{\sqrt{\rho\tau_\mathrm{p}}}\sum_{m=1}^{M}\tilde{\mathbf{w}}_{\mathrm{p},mk}^H\mathbf{g}_{mk'}\right|^2\right\} \\
&\underline{\underline{(h)}}\ \rho\eta_{k'}\sum_{m=1}^{M}\beta_{mk}\beta_{mk'}\mathrm{tr}(\mathbf{R}_{mk}\mathbf{R}_{mk'}) + \frac{\eta_{k'}}{\tau_\mathrm{p}}\sum_{m=1}^{M}\beta_{mk'}\mathrm{tr}(\mathbf{R}_{mk'}).
\end{aligned}$$

where in (g) we also utilized the fact in (a), while (h) can be obtained from that $\mathbf{g}_{mk}$ and $\mathbf{g}_{mk'}$ are independent and $\mathbf{h}_{mk'} \sim \mathcal{CN}(\mathbf{0}_N, \mathbf{R}_{mk'})$.

Finally, we compute $\mathbb{E}\left\{|\mathrm{NI}_k|^2\right\}$. From (11), we have

$$\begin{aligned}
&\mathbb{E}\left\{|\mathrm{NI}_k|^2\right\} \\
&= \mathbb{E}\left\{\left|\left(\sum_{m=1}^{M}\left(\mathbf{g}_{mk} + \frac{1}{\sqrt{\rho\tau_\mathrm{p}}}\tilde{\mathbf{w}}_{\mathrm{p},mk}\right)^H\mathbf{w}_{\mathrm{u},m}\right)\right|^2\right\} \\
&\underline{\underline{(i)}}\ \sum_{m=1}^{M}\beta_{mk}\mathrm{tr}\left(\mathbf{R}_{mk}\right) + \frac{MN}{\rho\tau_\mathrm{p}},
\end{aligned}$$

where (i) results from (20) and $\mathbf{w}_{\mathrm{p},mk} \sim \mathcal{CN}(0, \mathbf{I}_N)$.

REFERENCES

[1] V. W. Wong, R. Schober, D. W. K. Ng, and L.-C. Wang, *Key Technologies for 5G Wireless Systems*. Cambridge University Press, 2017.

[2] H. Ngo, A. Ashikhmin, H. Yang, E. Larsson, and T. Marzetta, "Cell-free massive MIMO versus small cells," *IEEE Trans. Wireless Commun.*, vol. 16, no. 3, pp. 1834–1850, Mar. 2017.

[3] J. Zhang, L. Dai, X. Li, Y. Liu, and L. Hanzo, "On low-resolution ADCs in practical 5G millimeter-wave massive MIMO systems," *IEEE Commun. Mag.*, vol. 56, no. 7, pp. 205–211, Jul. 2018.

[4] Z. Chen and E. Björnson, "Channel hardening and favorable propagation in cell-free massive MIMO with stochastic geometry," *IEEE Trans. Commun.*, vol. 66, no. 11, pp. 5205–5219, Jun. 2018.

[5] D. Maryopi, M. Bashar, and A. Burr, "On the uplink throughput of zero-forcing in cell-free massive MIMO with coarse quantization," *arXiv:1803.03608*, 2018.

[6] J. Zhang, Y. Wei, E. Björnson, Y. Han, and X. Li, "Spectral and energy efficiency of cell-free massive MIMO systems with hardware impairments," in *Proc. Int. Conf. Wireless Commun. Signal Process. (WCSP), Nanjing, China*, Oct 2017, pp. 1–6.

[7] J. Zhang, Y. Wei, E. Björnson, Y. Han, and S. Jin, "Performance analysis and power control of cell-free massive MIMO systems with hardware impairments," *IEEE Access*, vol. 6, pp. 55 302–55 314, 2018.

[8] M. Bashar, K. Cumanan, A. G. Burr, H. Q. Ngo, and H. V. Poor, "Mixed quality of service in cell-free massive MIMO," *IEEE Commun. Lett.*, vol. 22, no. 7, pp. 1494–1497, Jul. 2018.

[9] T. H. Nguyen, H. D. Han *et al.*, "Optimal power control and load balancing for uplink cell-free multi-user massive MIMO," *IEEE Access*, vol. 6, pp. 14 462–14 473, 2018.

[10] Y. Li and G. A. A. Baduge, "NOMA-aided cell-free massive MIMO systems," *IEEE Wireless Commun. Lett.*, vol. 7, no. 6, pp. 950–953, 2018.

[11] H. Q. Ngo, L. Tran, T. Q. Duong, M. Matthaiou, and E. G. Larsson, "On the total energy efficiency of cell-free massive MIMO," *IEEE Trans. Green Commun. Netw.*, vol. 2, no. 1, pp. 25–39, Mar. 2018.

[12] L. D. Nguyen, T. Q. Duong, H. Q. Ngo, and K. Tourki, "Energy efficiency in cell-free massive MIMO with zero-forcing precoding design," *IEEE Commun. Lett.*, vol. 21, no. 8, pp. 1871–1874, Aug. 2017.

[13] H. Yang and T. L. Marzetta, "Energy efficiency of massive MIMO: Cell-free vs. cellular," in *IEEE VTC Spring*. IEEE, 2018, pp. 1–5.

[14] M. Karlsson, E. Björnson, and E. G. Larsson, "Techniques for system information broadcast in cell-free massive MIMO," *IEEE Trans. Commun.*, vol. 67, no. 1, pp. 244–257, Jan. 2019.

[15] Ö. Özdogan, E. Björnson, and E. G. Larsson, "Massive MIMO with spatially correlated rician fading channels," *arXiv:1805.07972*, 2018.

[16] E. Björnson, J. Hoydis, and L. Sanguinetti, "Massive MIMO networks: Spectral, energy, and hardware efficiency," *Foundations and Trends® in Signal Processing*, vol. 11, no. 3-4, pp. 154–655, 2017.

[17] T. M. Hoang, H. Q. Ngo, T. Q. Duong, H. D. Tuan, and A. Marshall, "Cell-free massive MIMO networks: Optimal power control against active eavesdropping," *IEEE Trans. Commun.*, vol. 66, no. 10, pp. 4724–4737, Oct. 2018.

[18] J. Zhang, L. Dai, Z. He, B. Ai, and O. A. Dobre, "Mixed-ADC/DAC multipair massive MIMO relaying systems: Performance analysis and power optimization," *IEEE Trans. Commun.*, vol. 67, no. 1, pp. 140–153, Jan. 2019.

[19] J. Zhang, L. Dai, Z. He, S. Jin, and X. Li, "Performance analysis of mixed-ADC massive MIMO systems over Rician fading channels," *IEEE J. Sel. Areas Commun.*, vol. 35, no. 6, pp. 1327–1338, Jun. 2017.

[20] E. Björnson, M. Matthaiou, and M. Debbah, "Massive MIMO with non-ideal arbitrary arrays: Hardware scaling laws and circuit-aware design," *IEEE Trans. Wireless Commun.*, vol. 14, no. 8, pp. 4353–4368, Aug. 2015.